ELSEVIER

Journal of Molecular Catalysis A: Chemical 157 (2000) 97–109

JOURNAL OF MOLECULAR CATALYSIS A: CHEMICAL

www.elsevier.com/locate/molcata

Supported organometallic complexes. Part XX. Hydroformylation of olefins with rhodium(I) hybrid catalysts ☆

Ekkehard Lindner [a,*], Friedrich Auer [a], Andreas Baumann [a], Peter Wegner [a], Hermann A. Mayer [a], Helmut Bertagnolli [b], Ulrich Reinöhl [b], Teja S. Ertel [b], Achim Weber [b]

[a] *Institut für Anorganische Chemie der Universität Tübingen, Auf der Morgenstelle 18, D-72076 Tübingen, Germany*
[b] *Institut für Physikalische Chemie der Universität Stuttgart, Pfaffenwaldring 55, D-70569 Stuttgart, Germany*

Received 20 July 1999; received in revised form 30 November 1999; accepted 24 December 1999

Abstract

The rhodium(I) complexes $HRh(CO)[Ph_2P(CH_2)_xSi(OMe)_3]_3$ [**1a,b(T^0)$_3$**; **a**: $x = 3$, **b**: $x = 6$; T: T-type silicon atom, three oxygen neighbors] were sol–gel processed with the bifunctional cocondensation agent $(MeO)_3Si(CH_2)_6Si(OMe)_3$ **(T–C$_6$–T)** and in a separate reaction also with three additional equivalents of the phosphine ligand $Ph_2P(CH_2)_xSi(OMe)_3$ **[2a,b(T^0)]**. The resulting stationary phases **1a(T^n)$_3$(T^n–C$_6$–T^n)$_y$**, **1a(T^n)$_3$[2a(T^n)]$_3$(T^n–C$_6$–T^n)$_y$**, and **1b(T^n)$_3$[2b(T^n)]$_3$(T^n–C$_6$–T^n)$_y$** ($n = 0$–3, number of Si–O–Si bonds; ***y***: content of cocondensation agent) show a relatively narrow particle size distribution. The structural integrity of the rhodium complex **1** after the polycondensation was established by an EXAFS structure elucidation of the polysiloxane **1a(T^n)$_3$**. The obtained stationary phases proved to be efficient catalysts for the hydroformylation of 1-hexene in the presence of a wide variety of solvents in the interphase. Application of the materials containing non-coordinated ligands raised the selectivity toward hydroformylation up to 92% and the *n/iso* ratio to 14:1 with an average turnover number of 164 $mol_{sub}\ mol_{cat}^{-1}\ h^{-1}$. Higher olefins than 1-hexene were also hydroformylated with catalyst **D** and similar turnover frequencies and selectivities were obtained. ^{31}P CP/MAS NMR relaxation time studies (T_{PH}, $T_{1\rho H}$) were carried out in the presence (interphase) or absence (stationary phase) of a swelling solvent to investigate the dynamic behavior of the catalytically active polymer **1a(T^n)$_3$[2a(T^n)]$_3$(T^n–C$_6$–T^n)$_y$**. The highest mobility of the nonpolar reactive centers was achieved in nonpolar solvents like toluene, while more polar solvents like ethanol afforded the highest mobility of the overall polymer. (^{1}H,^{31}P) 2D WISE NMR experiments performed on the same material revealed a substantial decrease of the line width for the swollen polymer. ^{29}Si CP/MAS NMR experiments revealed a high degree of cross-linking and a larger content of cocondensation agent than introduced before condensation.

Keywords: Immobilized catalysts; Hydroformylation; Rhodium; Sol–gel; Solid-state NMR; EXAFS

1. Introduction

Among the homogeneously catalyzed industrial processes, hydroformylation is presently

☆ For Part XIX see Ref. [1].

* Corresponding author. Tel.: +49-7071-29-72039; fax: +49-7071-29-5306.

E-mail address: ekkehard.lindner@uni-tuebingen.de (E. Lindner).

1381-1169/00/$ - see front matter
PII: S1381-1169(00)00038-8

the most significant and the largest in scale [2,3], as it is used for the generation of more than 6 million tons of aldehydes per year [4]. Since Wilkinson's discovery of the catalytic activity and selectivity of the complex $HRh(PPh_3)_3(CO)$ in 1968 [5], rhodium-based systems have taken over a predominant position in hydroformylation. The application of such complexes in the presence of excess phosphine leads to selectivities for aldehyde formation of up to 99% and to *n*-aldehyde portions in the range of 95%. The only remaining problem of technical oxo processes is the separation of the precious catalyst from the reaction mixture. For the hydroformylation of propene, this task has been satisfactorily solved in the Ruhrchemie/Rhône-Poulenc process by application of a water-soluble catalyst acting in a two-phase reaction [6]. For long-chain olefins however, this method is not applicable due to the insolubility of such substrates in water. Thus, the synthesis of an easily separable catalyst for the hydroformylation of higher alkenes remains a challenge.

To achieve separability of homogeneous catalysts, many efforts have been made to anchor transition metal complexes to organic polymers [7–13] like cross-linked polystyrene or to the surface of inorganic supports like silica [14]. The major drawbacks of these concepts proved to be the limited thermodynamic stability of the organic matrices and the high degree of leaching of the silica-based systems [15a,15b].

A relatively new approach to the anchoring of catalyst complexes is their incorporation into a so-called interphase, in which a three-dimensional polymer framework (stationary phase) is permeated by a liquid or gaseous (mobile) phase. Herewith both phases are in contact on a molecular level, although no homogeneous mixture is formed. Thus, the state of the reactive centers in an idealized interphase is similar to that in solution.

Sol–gel condensed polysiloxanes [16–19a, 19b] have turned out to be useful as stationary phases, as they feature chemical and thermodynamic stability as well as a wide variability in mobility and polarity. Stationary phases consist of the matrix (polysiloxane), spacer groups (hydrocarbon chains) and the reactive center. Compared to functionalized silica, these systems offer the advantages of higher maximum metal complex loading and of lower leaching susceptibility [15a,15b]. In a recent study [20], we employed for the first time bifunctional alkoxydisilanes of the type $Me(MeO)_2Si–(CH_2)_z–Si(OMe)_2Me$ ($\mathbf{D^0–C_z–D^0}$, $z = 6, 8, 14$) in the sol–gel condensation of a transition metal complex. Such polysiloxane building-blocks are expected to combine efficient cross-linking and high flexibility of the matrix. A high flexibility of the polymer framework is necessary to achieve maximum mobility and consequently selectivity of the active centers [1].

In this work, the bifunctional cocondensation agent $(MeO)_3Si–(CH_2)_6–Si(OMe)_3$ ($\mathbf{T^0–C_6–T^0}$) was utilized because it provides a high degree of cross-linking together with a sufficient flexibility of the resulting polymer. Having demonstrated that the selective hydrogenation of a molecule as bulky as diphenyl ethyne is feasible in the interphase [21], we intented to transfer this concept to hydroformylation. The catalytically active center polycondensed for this purpose was a carbonylhydrido(trisphosphine)rhodium(I) complex with T-functionalized (T-type: silicon atom with three oxygen neighbors) diphenylphosphine ligands containing a three- or six-membered hydrocarbon spacer. Wieland and Panster [22] reported on the hydroformylation of 1-octene using a similar polysiloxane-bound rhodium complex with double spacer ligands and a monofunctional Q-type (silicon atom with four oxygen neighbors) cocondensation agent. Working in a continuous flow reactor with good turnover frequencies and long catalyst lifetime, this system suffered from an unsatisfactory *n/iso* ratio. Earlier attempts employing such an oxo catalyst complex grafted to functionalized organic polymers or to the surface of silica [23] resulted in similar *n/iso* ratios around 2:1.

The inorganic–organic hybrid materials described in this study were obtained by sol–gel condensation of the above mentioned complex with and without excess phosphine. Prior to the application in the hydroformylation, the new materials were characterized by IR and CP/MAS NMR spectroscopy and by an EXAFS structure determination.

2. Experimental

2.1. Reagents and physical measurements

$RhCl_3 \cdot 3H_2O$ was a gift from Degussa. Si(OEt)$_4$ was obtained from Aldrich; *cis*-cyclooctene, 1-hexene, 1-decene, and 1-tetradecene were received from Merck and $Cl(CH_2)_3Si(OMe)_3$ from ABCR. The T-functionalized phosphine ligands $Ph_2P(CH_2)_x$–$Si(OMe)_3$ **[2a,b(T^0)]** [24a,24b] were synthesized as described. 1,6-Bis(trimethoxysilyl)hexane **(T^0–C$_6$–T^0)** was synthesized in analogy to the **D^0–C$_x$D^0** cocondensation agents reported recently [21].

Elemental analyses were carried out on a Carlo Erba Analyzer, Model 1106. IR data were obtained on a Bruker IFS 48 FT-IR spectrometer. Scanning electron micrographs were recorded on a Zeiss DSM 962 with a tungsten cathode (4.5 nm diameter). The samples were sputtered with platinum to form layers of 10-nm thickness and measured at a beam voltage of 30 kV. The surface areas were determined by nitrogen sorption and calculated with the BET equation on a Micrometrics Gemini 2375. The rhodium content was measured by atomic absorption spectrometry on a Varian SpectrAA 20 Plus spectrometer. The polymer samples were dissolved by stirring in 5 ml of a concentrated NaOH solution and subsequently diluted to 100 ml.

Solution NMR spectra were recorded on a Bruker DRX 250 and Bruker AC 80 spectrometer at 298 and 306 K, respectively. Frequencies and standards were as follows: $^{31}P\{^1H\}$ NMR: 101.25 and 32.44 MHz, external standard 85% H_3PO_4/D_2O; $^{13}C\{^1H\}$ NMR: 62.90 MHz; ^1H NMR: 250.13 MHz. All ^1H and $^{13}C\{^1H\}$ NMR spectra were calibrated relative to partially deuterated solvent peaks which are reported relative to tetramethylsilane (TMS).

The CP/MAS solid state NMR spectra were recorded on a Bruker MSL 200 (^{29}Si) and a Bruker ASX 300 (^{13}C and ^{31}P) multinuclear spectrometer equipped with wide bore magnets (field strengths: 4.7 and 7.05 T, respectively). Magic angle spinning was applied at 3 kHz (^{29}Si) and 10 kHz (^{31}P, ^{13}C). All measurements were carried out under exclusion of molecular oxygen. Frequencies and standards: ^{29}Si, 39.75 MHz [TMS, the trimethylester of double four-ring octameric silicate Q_8M_8 ($\delta(^{29}Si)$ of the M group was set to 12.3 ppm) as secondary standard [25a,25b]; ^{13}C, 75.47 MHz [TMS, carbonyl resonance of glycine (δ 176.03) as the second standard]; ^{31}P, 121.49 MHz [85% H_3PO_4, $NH_4H_2PO_4$ (δ 0.8) as the second standard]. The cross polarization constants T_{PH} and T_{SiH} were determined by variations of the contact time (20–25 experiments). The proton relaxation time in the rotating frame $T_{1\rho H}$ was measured by direct proton spin lock-τ-CP experiments as described by Schaefer et al. [26]. T_{1P} values were received using the method developed by Torchia [27]. The relaxation time data were obtained by using the Bruker software SIMFIT or Jandel software PEAKFIT. Peak deconvolution of the spectra was performed with the Bruker-Spectrospin software SNMR using Voigtian line shapes. The T_{SiH} values of 0.92, 0.91 and 1.15 ms for the T^1, T^2, and T^3 groups, respectively and $T_{1\rho H}$ of 3.69 ms were used to calculate the realistic intensities of the **T^n** species. The WISE NMR spectra were recorded under MAS conditions (3 kHz). Sixty-four t_1 increments with a dwelling time of 3–10 μs were used for each spectrum. Cross polarization was applied with contact times of 200 μs for WISE experiments to eliminate spin-diffusion

effects and of 2–5 ms for CP/MAS experiments, respectively.

The EXAFS measurements of **1a(T^0)$_3$** were performed at the beamline A1 of the Hamburger Synchrotronstrahlungslabor (HASYLAB) at DESY, Hamburg, at the rhodium K-edge (23 224.0 eV) under ambient conditions (5.6 GeV, beam current 100 mA). Data were collected in transmission mode with ion chambers flushed with argon. The second crystal of the Si⟨311⟩ double crystal monochromator was set as to obtain 30% harmonic rejection. For data acquisition the energy was scanned over a range of 23000–24400 eV. Energy calibration was monitored by a rhodium foil of 20 μm thickness. The sample itself was prepared by pressing a mixture of **1a(T^0)$_3$** and polyethylene in a mass ratio of 4:1 to a tablet of 13 mm diameter and 3.0 mm thickness, stored under an inert gas atmosphere and measured on air exposure at room temperature. Data reduction was performed with a program package especially developed for the requirements of amorphous samples [28]. Background subtraction was performed with AUTOBK (University of Washington) [29], and data were analyzed with the EXCURV92-module [30] of ''CERIUS2''. The amplitude reduction factor AFAC was fixed at 0.8, and an overall energy shift E_f was introduced to obtain the best fit to the data.

The hydroformylation experiments were carried out in a 100-ml autoclave under exclusion of oxygen. The analyses were performed on a GC 6000 Vega Series 2 (Carlo Erba Instruments) with a FID and a capillary column PS 255 [13.5 m; carrier gas, He (40 kPa); integrator 3390 A (Hewlett Packard)].

All manipulations were performed under argon by employing the usual Schlenk techniques. Methanol was dried with magnesium and distilled, ethanol was distilled from NaOEt. *n*-Hexane and toluene were distilled from sodium benzophenone ketyl, acetone was distilled from P_4O_{10}, water was distilled under argon prior to use.

2.2. Preparation of the momomeric and polycondensed rhodium(I) complexes

The monomeric rhodium complexes H(CO)Rh[$Ph_2P(CH_2)_xSi(OMe)_3$]$_3$ ($x = 3$, 6) **[1a,b(T^0)$_3$]** were prepared according to known synthetic procedures [31] from [μ-ClRh(COE)$_2$]$_2$ (COE = cyclooctene) and the ligands $Ph_2P(CH_2)_xSi(OMe)_3$ ($x = 3$, 6) **[2a,b(T^0)]** [24a, 24b] with subsequent carbonylation and reduction of the carbonylchlororhodium intermediate with $NaBH_4$ in ethanol at ambient temperature.

Carbonyltris[diphenyl(trimethoxysilylpropyl)-phosphine]hydridorhodium(I) **[1a(T^0)$_3$].** $^{31}P\{^1H\}$ NMR (32.391 MHz, EtOH, −30°C): δ 28.2 (d, ^1J(RhP) = 150.9 Hz). IR (KBr, cm^{-1}): 1967 [ν(CO)].

Carbonyltris[diphenyl(trimethoxysilylhexyl)-phosphine]hydridorhodium(I) **[1b(T^0)$_3$[.** $^{31}P\{^1H\}$ NMR (101.259 MHz, EtOH, 20°C): δ 30.0(d, ^1J(RhP) = 151.5 Hz). IR (KBr, cm^{-1}): 1967 [ν(CO)].

Table 1
Labeling of the polycondensation products

Educt	Excess ligand/amount	Cocondensation agent/amount	Product labeling	Material
HRh(CO)(P–C_3–T^0)$_3$ **[1a(T^0)$_3$]**			**1a(T^n)$_3$**	**A**
HRh(CO)(P–C_3–T^0)$_3$ **[1a(T^0)$_3$]**		$(MeO)_3Si(CH_2)_6Si(OMe)_3$ **[T^0–C_6–T^0]**/4	**1a(T^n)$_3$(T^n–C_6–T^n)$_y$**	**B**
HRh(CO)(P–C_3–T^0)$_3$ **[1a(T^0)$_3$]**	P–C_3–T^0 **[2a(T^0)]**/3	$(MeO)_3Si(CH_2)_6Si(OMe)_3$ **[T^0–C_6–T^0]**/4	**1a(T^n)$_3$[2a(T^n)]$_3$(T^n–C_6–T^n)$_y$**	**C**
HRh(CO)(P–C_6–T^0)$_3$ **[1b(T^0)$_3$]**	P–C_6–T^0 **[2b(T^0)]**/3	$(MeO)_3Si(CH_2)_6Si(OMe)_3$ **[T^0–C_6–T^0]**/4	**1b(T^n)$_3$[2b(T^n)]$_3$(T^n–C_6–T^n)$_y$**	**D**

Carbonyltris[diphenyl(polysiloxanylpropyl)-phosphine]hydridorhodium(I) **[1a(T^n)$_3$, A,** see also Table 1]. To a solution of 983 mg (0.836 mmol) of **1a(T^0)$_3$** in ethanol (35 ml) 2 ml of degassed water was added. The mixture was heated to 50°C and stirred over 3 h, then it was evaporated to dryness to yield a pale yellow gel. As the product is partially soluble in acetone and Et_2O and readily soluble in toluene, the washing procedure was renounced. Yield: 687 mg (84.2%). Anal. Calcd for $C_{46}H_{55}O_{4.5}P_3RhSi_3$:[1] C, 57.55; H, 5.77; Rh, 10.72. Found: C, 56.86; H, 5.64; Rh, 10.38. IR (KBr, cm^{-1}): 1967 [ν (CO)].

Carbonyltris[diphenyl(polysiloxanylpropyl)-phosphine]hydridorhodium(I) **(T^n–C_6–T^n)$_y$ [1a(T^n)$_3$(T^n–C_6–T^n)$_y$, B]**. To a solution of 983 mg (0.836 mmol) of **1a(T^0)$_3$** in ethanol (35 ml) 1.09 g (3.34 mmol) of 1,6-bis(trimethoxysilyl)hexane **(T^0–C_6–T^0)** and 2 ml of degassed water were added. The mixture was stirred and heated to 50°C. After 3 h a yellow precipitate was formed. The suspension was evaporated to dryness and washed with 10 ml each of *n*-hexane, Et_2O, THF, acetone, ethanol, methanol, water, methanol, ethanol, acetone, THF, Et_2O, and toluene to remove any soluble products. Finally, the polycondensate was dried at room temperature in vacuo for 3 h to yield a pale yellow powder. Yield: 1.286 g (88.9%). Anal. Calcd for $C_{70}H_{103}O_{17.5}P_3RhSi_{11}$ (idealized stoichiometry):[1] C, 48.62; H, 6.00; Rh, 5.95; for $C_{85}H_{134}O_{28.5}P_3RhSi_{16}$ (corrected stoichiometry):[2] C, 45.23; H, 5.98; Rh, 4.56. Found: C, 44.55; H, 5.97; Rh, 4.02. ^{31}P CP/MAS NMR: δ 29. ^{13}C CP/MAS NMR: δ 138–119 (Ph), 31.3 ($SiCH_2CH_2\mathit{C}H_2$), 22.9 ($SiCH_2\mathit{C}H_2$), 13.2. ($SiCH_2$). ^{29}Si CP/MAS NMR: (−59.7 (T^2), −66.9 (T^3). IR (KBr, cm^{-1}): 1964 [ν(CO)]. N_2 surface area: 0.60 $m^2\ g^{-1}$.

Preparation of the carbonylhydrido(trisphosphine)rhodium(I) complexes **C** and **D** polycondensed with additional phosphine. To a solution of 983 mg (0.836 mmol) of **1a(T^0)$_3$** [or 1.094 g (0.84 mmol) of **1b(T^0)$_3$**] in ethanol (35 ml) 875 mg (2.51 mmol) of **2a(T^0)** [or 984 mg (2.52 mmol) of **2b(T^0)**], 1.09 g (3.34 mmol) of 1,6-bis(trimethoxysilyl)hexane **(T^0–C_6–T^0)**, and 2 ml of degassed water were added. The mixture was stirred and heated to 50°C. After 3 h, a yellow precipitate was formed. Working up in analogy to **B** (vide supra) afforded **C** and **D** as pale yellow and pale orange powders, respectively.

Blend of carbonyltris[diphenyl(polysiloxanylpropyl)phosphine]hydridorhodium(I) **(T^n–C_6–T^n)$_y$** and diphenyl(polysiloxanylpropyl)-phosphine**(T^n–C_6–T^n)$_y$ {1a(T^n)$_3$[2a(T^n)]$_3$-(T^n–C_6–T^n)$_y$, C}.** Yield: 1.92 g (89.2%). Anal. Calcd for $C_{115}H_{157}O_{22}P_6RhSi_{14}$ (idealized stoichiometry):[1] C, 53.67; H, 6.15; Rh, 4.00; for $C_{131.8}H_{183.6}O_{32.9}P_6RhSi_{19.6}$ (corrected stoichiometry):[2] C, 50.52; H, 5.90; Rh, 3.28. Found: C, 50.61; H, 5.96; Rh, 2.82. ^{31}P CP/MAS NMR: δ 29 (Rh–PPh_2), −18 (PPh_2). ^{13}C CP/MAS NMR: δ 138–119 (Ph), 31.7 ($SiCH_2CH_2\mathit{C}H_2$), 23.7 ($SiCH_2\mathit{C}H_2$), 14.9 ($SiCH_2$). ^{29}Si CP/MAS NMR: δ −58.8 (T^2), −66.0 (T^3). IR (KBr, cm^{-1}): 1968 [ν(CO)]. N_2 surface area: 2.06 $m^2\ g^{-1}$.

Blend of carbonyltris[diphenyl(polysiloxanylhexyl)phosphine]hydridorhodium(I) **(T^n–C_6–T^n)$_y$** and diphenyl(polysiloxanylhexyl)-phosphine**(T^n–C_6–T^n)$_y$ {1b(T^n)$_3$[2b(T^n)]$_3$(T^n–C_6–T^n)$_y$, D}**. Yield: 2.122 g (89.4%). Anal. Calcd for $C_{133}H_{193}O_{22}P_6RhSi_{14}$ (idealized stoichiometry):[1] C, 56.53; H, 6.88; Rh, 3.64; for $C_{149.2}H_{218.8}O_{32.8}P_6RhSi_{19.4}$ (corrected stoichiometry):[1] C, 53.16; H, 6.54; Rh, 3.05. Found: C, 53.69; H, 6.50; Rh, 2.69. ^{31}P CP/MAS NMR: δ 29 (Rh–PPh_2), −18 (PPh_2). ^{13}C CP/MAS NMR: δ 138 − 119 (Ph), 32.1 ($SiCH_2CH_2\mathit{C}H_2\mathit{C}H_2\mathit{C}H_2\mathit{C}H_2$–$PPh_2$), 23.3 ($SiCH_2\mathit{C}H_2$), 13.7 ($SiCH_2$). ^{29}Si CP/MAS

[1] The given formula is the repeating unit of a polymer.

[2] The corrected stoichiometries were obtained by considering the cocondensation agent content as derived from the ^{13}C CP/MAS NMR measurements. The incomplete condensation was also taken into account by adding the additional number OH groups to the formula.

NMR: δ −58.7 **(T^2)**, −66.4 (T^3). IR (KBr, cm^{-1}): 1967 [ν(CO)]. N_2 surface area: 1.05 m^2g^{-1}.

3. Results and discussion

*3.1. Preparation of the polycondensed carbonylhydridorhodium(I) complexes **1***

Addition of water and the cocondensation agent **T^0–C_6–T^0** to a solution of **1a(T^0)$_3$** in ethanol and heating the mixture to 323 K resulted in the precipitation of the yellow polycondensate **B** (Scheme 1, Table 1). In alternative experiments, excess ligand **2a,b(T^0)** was added immediately after the generation of the carbonylhydridorhodium(I) complexes **1a,b(T^0)$_3$**, with formation of the polymeric complexes **C** and **D** as stationary phases (Scheme 1, Table 1). The sol–gel process was sufficiently catalyzed by $NaBH_4$, therefore no additional condensation catalyst, such as HCl, NaOH or $(nBu)_2Sn(OAc)_2$, had to be employed. The idealized and realistic composition of the polycondensates are summarized in Scheme 2.

Several characterization methods verify the structural integrity of the rhodium complex centers in **B, C,** and **D** after the polycondensation: the CO absorptions in the FT-IR spectra of the monomeric precursors **1a,b(T^0)$_3$** and the polymeric complexes are identical (see Section 2).

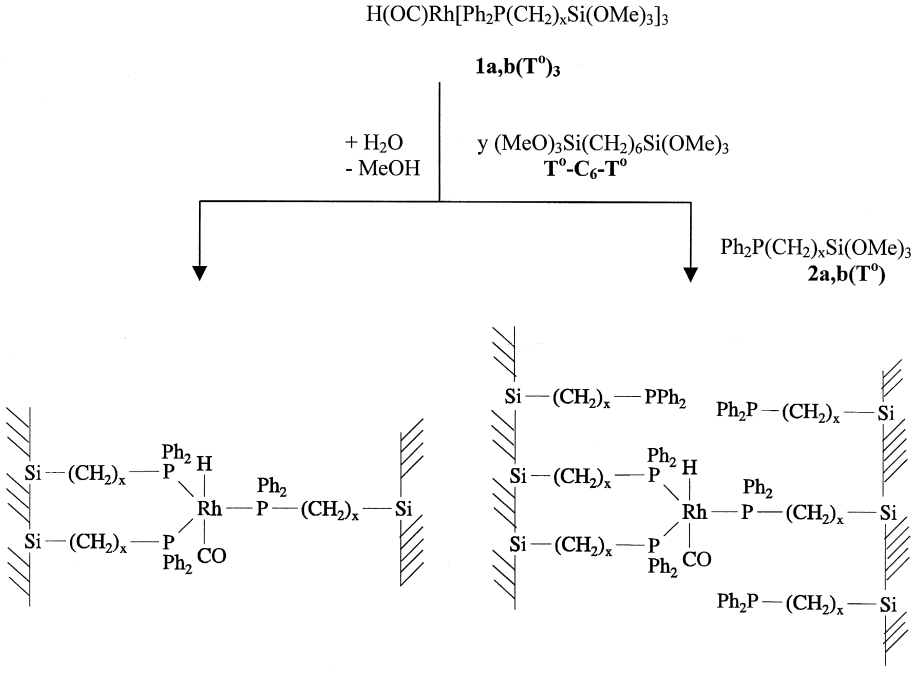

1a(T^n)$_3$ (A)
1a(T^n)$_3$(T^n-C_6-T^n)$_y$ (y = 4) **(B)**

1a(T^n)$_3$ [2a(T^n)$_3$](T^n-C_6-T^n)$_y$ (y = 4) **(C)**
1b(T^n)$_3$ [2b(T^n)$_3$](T^n-C_6-T^n)$_y$ (y = 4) **(D)**

x	3	6
	a	**b**

T^n : T type silicon atom (three oxygen neighbors)
n = 0 – 3 (number of Si-O-Si bonds)

Scheme 1.

Idealized polycondensation

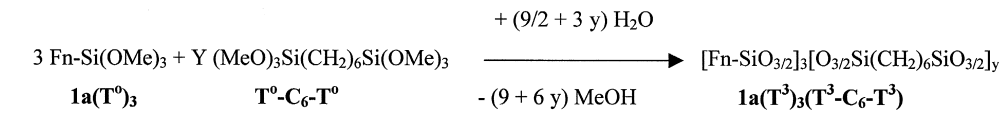

Realistic composition of the polycondensate

$[Fn\text{-}SiO_{n/2}(OX)_{3-n}]_3[O_{n/2}(XO)_{3-n}Si(CH_2)_6Si(OX)_{3-n}O_{n/2}]_y$

$1a(T^n)_3(T^n\text{-}C_6\text{-}T^n)$

Fn = $(HRhCO)_{1/3}Ph_2P(CH_2)_6$-

T^n : T type silicon atom (three oxygen neighbors)

n = 0 – 3 (number of Si-O-Si bonds)

X = H, Me

y = amount of the incorporated co-condensation agent

Scheme 2.

The ^{31}P CP/MAS NMR spectrum of the polycondensed complex **B** features only one signal in the chemical shift region of its monomeric congener. For the materials containing additional phosphine ligands of the type **2a,b(T^0)**, a further ^{31}P resonance is observed at a chemical shift which is typical for this type of ligand in solution (see Fig. 1).

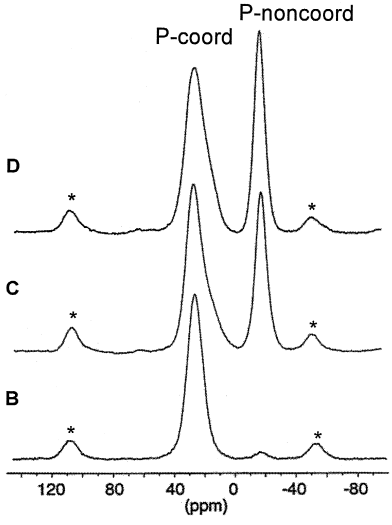

Fig. 1. ^{31}P CP/MAS NMR spectra of the copolymerized rhodium complexes **1**. Spinning side bands are denoted as asterisks. P-coord and P-noncoord refer to the coordinated and non-coordinated phosphine ligands, respectively.

*3.2. EXAFS structure determination of the polycondensed rhodium(I) complex **A***

Since the polycondensates **1** are amorphous, their structure cannot be determined by X-ray diffraction methods. However, EXAFS spectroscopy represents a convenient method to obtain information on the atomic environment of a given absorber atom, independent of the sample's physical state. The polymer investigated in this experiment was synthesized in the absence of any cocondensation agent to provide the highest possible rhodium loading. Data evaluation revealed the coordination of one carbonyl molecule and of three equivalent phosphine ligands to the metal center, thus confirming the preservation of the molecular geometry around the metal center in **A** after polycondensation. To optimize the fitting to the experimental EXAFS spectrum it is necessary to take multiple scattering effects into account. Therefore the carbonyl ligand was defined as one backscattering unit. The analysis led to the structural parameters given in Table 2. The experimental and the calculated $k^3\chi(k)$ function as well as their Fourier transforms are shown in Fig. 2. The rhodium phosphorus bond distance (232 pm) was found to be in the same range as for the

Table 2
Spectroscopically determined structural data absorber–backscatterer distance [Å], coordination number, and Debye–Waller factor σ [Å] of material **A** (errors of r and N given in parentheses), energy shift $E_f = 0.7 \pm 0.3$

	r [Å]	N	σ [Å]
Rh–C	1.77 (±0.02)	1 (±0.2)	0.050 (±0.01)
Rh–P	2.32 (±0.02)	3 (±0.6)	0.077 (±0.03)
Rh–O[a]	2.95 (±0.02)	1 (±0.2)	0.059 (±0.02)

[a] Distance of the Rh–C–O bond.

analogous Wilkinson complex $HRh(PPh_3)_3(CO)$ [32]. The metal carbon bond, however, is shortened to 177 pm (compared to 181 pm) owing to a stronger bonding of the carbonyl to the rhodium atom attached to the more basic alkyldiphenylphosphine ligands **2a(T^0)**.

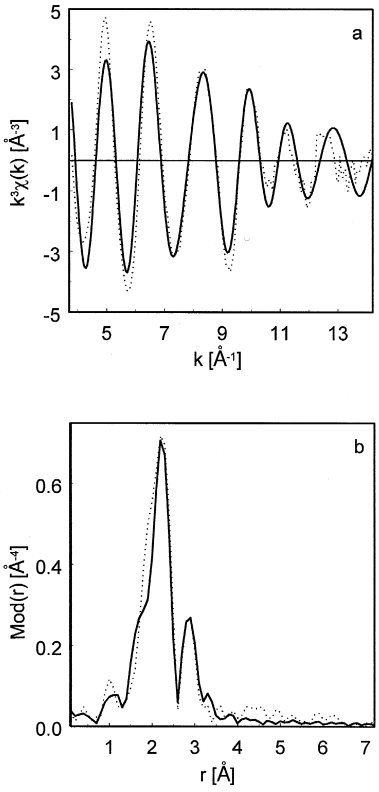

Fig. 2. Calculated (solid line) and experimental (dotted line) $k^3\chi(k)$ function (a) and their Fourier transforms (b) (Rh–K–edge) in the k-range of 3–14.6 Å^{-1}.

3.3. SEM investigations of the polycondensed carbonylhydridorhodium(I) complexes *B*, *C*, and *D*

The scanning electron micrographs, in particular of the polycondensates **B**, **C**, and **D** (Fig. 3a,b) revealed a relatively narrow particle size distribution. Most particles are in the range between 10 and 20 μm. The SEM micrographs of all T–C_6–T copolymers featured an even surface structure without any porosity, which is in good agreement with the low specific surfaces of these materials obtained by BET measurements. Small deposits on their surfaces are

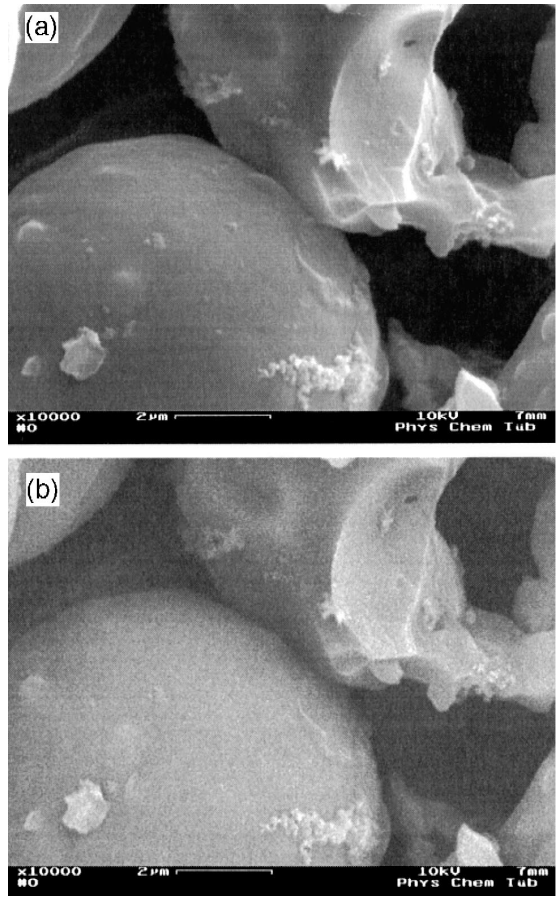

Fig. 3. Scanning electron micrographs of the polysiloxanes after hydroformylation (a), and backscattering electron micrograph of the polysiloxane *B* after hydroformylation (b).

attributed to the polycondensation of yet uncondensed siloxanes during the evaporation of the solvent. Slight differences in the surface curvature of the polycondensates **B**, **C**, and **D** are explained by differences in the polarity of these materials leading to different surface energies of the polysiloxane particles during the sol–gel transition. A sample of the complex **B** which was investigated after hydroformylation did not show any significant change of the particle shape, size, and surface structure (Fig. 3a). No indication for the generation of metal particles on the polymer surface [19a,19b] was found, as a backscattering experiment did not reveal spots of higher electric conductivity (Fig. 3b).

*3.4. ^{29}Si, ^{31}P, and ^{13}C CP / MAS NMR characterization of the polymers **B**, **C**, and **D***

The ^{29}Si CP/MAS NMR spectra of the above mentioned copolymers revealed two broad signals. They are typical for $\mathbf{T^2}$ and $\mathbf{T^3}$ silicon atoms, corroborating an efficient condensation of the silanol groups. Absorptions attributable to $\mathbf{T^1}$ species were very weak, while $\mathbf{T^0}$ moieties did not occur in an appreciable extent. It is noteworthy that the ^{29}Si NMR signal patterns of these copolymers resemble the one obtained by Oviatt et al. [33] from a material synthesized by polycondensation of pure 1,6-bis(trimethoxysilyl)hexane.

In order to obtain realistic intensities of the $\mathbf{T^n}$ species (Table 3) the ^{29}Si CP/MAS NMR spectra were quantified as described earlier [34]. A high degree of condensation was observed.

Table 3
Relative intensities of the silyl species in the copolymers

Matrices	Relative intensities of the Si groups (%)			Degree of condensation (%)
	$\mathbf{T^1}$	$\mathbf{T^2}$	$\mathbf{T^3}$	
B	2.0	60.4	37.5	78.4
C	2.6	33.2	64.2	87.2
D	–	42.2	57.8	85.9

Table 4
$T_{1\rho H}$ and T_{PH} values of the material **C** with and without a solvent

	$T_{1\rho H}$ [ms]	T_{PH} (ligand) [ms]	T_{PH} (complex) [ms]
Dry	7.1	0.37	0.27
Toluene	6.71	1.0	0.54
Ethanol	4.62	0.54	0.4

As the ^{29}Si NMR chemical shifts of the silyl functionalities in the ligand and in the cocondensation agent (T-groups) are identical, the metal/cocondensation agent ratio within the polymer cannot be determined by means of ^{29}Si CP/MAS NMR spectroscopy. The only way to estimate the content of $\mathbf{T^n–C_6–T^n}$ in the polycondensate is to compare the corrected integrals of the phenyl signals with those of the aliphatic signals in the ^{13}C CP /MAS NMR spectra of the cocondensates. Such evaluation of the measured data resulted in y values of 6.5, 6.8 and 6.7 for the cocondensates **B**, **C**, and **D**, respectively. As this method does not allow but a coarse estimation of the polymer composition, these materials are hereafter denoted as **B**, **C**, and **D**. The corrected y values are taken into account in the elemental analyses of these polymers (see Experimental Section).

In the ^{31}P CP/MAS NMR spectra of the above mentioned materials (Fig. 1) only the expected signals characteristic for the HRh(CO)P_3 complex and — in the cases of **C** and **D** — also for the non-coordinated phosphines are observed. The ^{31}P resonances of the non-coordinated P ligands (δ −18) feature a perceivably smaller line width than the ^{31}P complex signals (δ + 29) owing to the higher mobility and to the smaller chemical shift dispersion of the ligands. ^{31}P CP/MAS NMR spectra of **C** measured in suspension using ethanol or toluene as solvent (as a mobile phase) show a significant decrease of the line width of the non-coordinated phosphine signals, which is a consequence of the increased mobility of these groups within the swollen polymer. Elucidation of the relaxation times by a contact time variation resulted in the

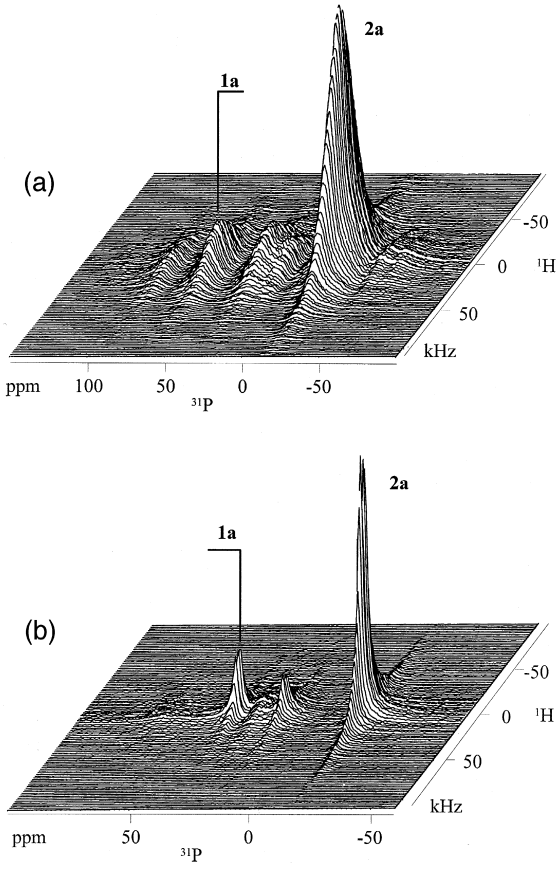

Fig. 4. (^{1}H,^{31}P) 2D WISE NMR spectra of the dry polymer **C** (a), and of the polymer **C** swollen in ethanol (b).

$T_{1\rho H}$ and T_{PH} (see Section 2.1) values shown in Table 4. The observed decrease of the $T_{1\rho H}$ values and the increase of the T_{PH} values for the swollen polymer is a further confirmation that the mobility in an interphase is higher than in a neat stationary phase. The lowest $T_{1\rho H}$ value, a magnitude characteristic for the mobility of the overall polymer, is obtained for EtOH, because polysiloxanes swell best in solvents of medium polarity. High T_{PH} values, however, are characteristic for a high mobility of the respective phosphorus containing functional groups. Since both the non-coordinated diphenylphosphine groups and the carbonylhydrido(trisphosphine)rhodium(I) complex constitute nonpolar groups, their state is most solution-like in nonpolar solvents.

A further valuable method to demonstrate differences in the mobility of the functional groups grafted to a polymer is the two-dimensional ''wideline-separation'' (2D WISE) NMR spectroscopy [35]. The broad lines of ^{1}H NMR spectroscopy would usually lead to superimposed lines in solid state NMR spectra. In the 2D WISE NMR spectroscopy this problem is solved by introducing a second dimension (^{31}P, Fig. 4). Comparison of the (^{1}H,^{31}P) 2D WISE NMR spectrum of the dry polymer **C** with the one measured in the presence of ethanol (Fig. 4a and b, respectively) reveals a substantial decrease of the line width in the ^{1}H dimension for the swollen gel, which, again, is more pronounced for the non-coordinated ligand than for the complex.

3.5. Catalytic hydroformylation of 1-hexene in the interphase

The polysiloxane-bound rhodium(I) complex **B** which is denoted as a stationary phase was

Table 5
Influence of the solvent on conversion and selectivity of 1-hexene hydroformylation with catalyst **B**
Reaction conditions: 373 K, 10 bar H_2, 10 bar CO, 150 min, 20 ml solvent, 20 mmol hexene (= 2.5 ml), 20 μmol catalyst **B**.

Solvent	Conversion (%)	Isomerization (%)	Hydrogenation (%)	Hydroformylation (%)	*n*/*n* + *iso* (%)	TON[a]
Toluene	52.15	31.8	1.2	67.0	73.0	521
THF	52.54	19.3	1.0	79.7	75.0	525
Acetone	38.93	10.2	1.7	88.1	77.5	389
Ethanol	58.64	12.7	2.3	85.0	84.7	586
Methanol	85.46	19.5	–	80.5	76.7	854
Water	50.24	20.6	2.3	77.1	69.7	502

[a] Turnover number (mol_{sub} mol_{cat}^{-1}).

Table 6
Influence of temperature and H_2/CO partial pressures on conversion and selectivity of 1-hexene hydroformylation with catalyst **B**
Reaction conditions: 150 min, 20 ml ethanol, 20 mmol hexene (= 2.5 ml), 20 μmol catalyst **B**.

Temperature (K)	$p(H_2)/p(CO)$ (bar)	Conversion (%)	Isomerization (%)	Hydrogenation (%)	Hydroformylation (%)	$n/n+iso$ (%)	TON[a]
353	10/10	49.21	19.4	1.0	79.6	71.4	492
373	10/10	58.64	12.7	2.3	85.0	84.7	586
393	10/10	77.22	67.3	20.6	12.1	96.9	772
373	15/5	87.7	25.9	42.1	32.0	94.3	877

[a]Turnover number ($mol_{sub}\ mol_{cat}^{-1}$).

able to catalyze the hydroformylation of 1-hexene with good turnover frequencies and fair selectivities in solvents (as a mobile phase) of different polarity from toluene to water (Table 5). Applying commonly used oxo reaction conditions (373 K, 10 bar H_2, 10 bar CO), polar solvents like MeOH afforded the highest activities, whereas the selectivity toward the formation of 1-heptanal was optimal in solvents of medium polarity like EtOH or acetone. Variation of the temperature and partial pressures (vide supra and Table 6) did not lead to an increase of selectivity, because lower temperatures caused a decrease of the *n/iso* ratio of the resulting aldehydes, whereas both higher temperatures and hydrogen partial pressures resulted in a dramatic increase of olefin isomerization and hydrogenation.

3.6. Application of catalyst with excess phosphine

In order to obtain a catalytically active material with a higher selectivity toward the generation of the desired linear aldehyde, an excess of three equivalents of the phosphine ligand **2a(T^0)** was added to the complex **1a(T^0)$_3$** prior to polycondensation. Indeed, the resulting compound **C** (Scheme 1) afforded a substantial improvement of the selectivity (Table 7). Under identical reaction conditions both the aldehyde portion and the $n/n+iso$ ratio increased from about 85% to 93%, accompanied by a slight drop of the activity. This effect of selectivity enhancement by addition of excess phosphine ligand has been observed many times for ligand modified oxo catalysts and can be explained by an equilibrium shift of the catalytically active species in favor of the highly selective diphosphine(carbonyl)hydridorhodium(I) species $(R_3P)_2Rh(CO)H$ over the less selective phosphinedicarbonyl complex $(R_3P)Rh(CO)_2H$ [36]. Since the initial step of the hydroformylation process is a phosphine ligand dissociation from the trisphosphine complex, the presence of excess ligand at the same time gives rise to a slightly reduced reaction rate.

Application of a phosphine with six instead of three spacer carbon atoms was expected to afford a higher mobility and thus an improved

Table 7
Influence of the catalyst on conversion and selectivity of 1-hexene hydroformylation
Reaction conditions: 373 K, 10 bar H_2, 10 bar CO, 150 min, 20 ml ethanol, 20 mmol hexene (= 2.5 ml), 20 μmol catalyst.

Catalyst	Conversion (%)	Isomerization (%)	Hydrogenation (%)	Hydroformylation (%)	$n/n+iso$ (%)	TON[a]
B	58.64	12.7	2.3	85.0	84.7	586
C	40.99	5.0	2.6	92.4	93.4	410
D	29.61	6.2	2.9	90.9	86.4	296

[a]Turnover frequency ($mol_{sub}\ mol_{cat}^{-1}\ h^{-1}$).

Table 8
Hydroformylation of long-chain olefins with complex D
Reaction conditions: 373 K, 10 bar H_2, 10 bar CO, 150 min, 20 ml ethanol, 20 mmol alkene, 20 μmol catalyst **D**.

1-Alkene	Conversion (%)	Isomerization (%)	Hydrogenation (%)	Hydroformylation (%)	$n/n+iso$ (%)	TON[a]
1-hexene	29.61	6.2	2.9	90.9	86.4	296
1-decene	29.0	3.4	3.7	92.0	84	290
1-tetradecene	20.55	2.7	1.2	96.1	84.9	206

[a] Turnover number ($mol_{sub}\ mol_{cat}^{-1}$).

selectivity. In agreement with earlier investigations by Pittman [11] the $n/n+iso$ ratio and the turnover frequencies obtained in the 1-hexene hydroformylation with complex **D** were inferior to those observed with the analogous material **C** which contains the short-chain ligand **2a(T^0)** (Table 7). In solvent swollen **C** the actual concentration (mmol of P per volume unit of swollen catalyst bead) of phosphine functions is higher than in **D** (constant P/Rh ratio). Like in Pittman's work the $n/n+iso$ ratio is increased at a constant P/Rh ratio as the overall density (concentration) of the P functions within the swollen polymer is increased.

In the presence of ethanol, complex **D** proved to be applicable also in the hydroformylation of 1-decene and 1-tetradecene with excellent selectivities (Table 8).

4. Conclusion

In this study we have demonstrated that rhodium(I) complexes acting as hydroformylation catalysts can be incorporated into a polysiloxane matrix by the sol–gel method. The polycondensation of monomeric species with the bifunctional cocondensation agent **T^0–C_6–T^0** resulted in flexible, but highly cross-linked inorganic–organic hybrid polymers as stationary phases with a relatively narrow particle size distribution. An EXAFS study proved the structural integrity of the complex centers within the polymer. In the hydroformylation of 1-hexene in the interphase, the cocondensates are active in a wide variety of solvents. The highest turnover numbers are obtained in polar solvents, while selectivities are best in solvents of medium polarity. This observation is rationalized by the fact that the swelling of the hybrid polymers — and therefore the mobility of the reactive centers — is best in medium polar solvents like ethanol, which was demonstrated by NMR studies of swollen polysiloxanes. Cocondensation of excess non-coordinated phosphine with the monomeric catalyst precursor and the cocondensation agent yielded stationary phases which afforded a substantial increase of selectivity toward the generation of *n*-aldehydes, a result that is explained by an equilibrium shift of the catalytically active species under the increased phosphine ligand concentration. The hydroformylation of the higher olefins 1-decene and 1-tetradecene was most efficiently catalyzed when a polymer containing phosphine ligand with hexyl instead of propyl spacers was employed. The smaller polarity and the larger mesh width of this material allows a better penetration by the big, lipophilic olefin molecules.

Acknowledgements

The support of this research by the Deutsche Forschungsgemeinschaft (Forschergruppe, Grant No. 154/41-4) Bonn, Bad Godesberg, and by the Fonds der Chemischen Industrie, Frankfurt/Main is gratefully acknowledged. We are grateful to Degussa, Germany for a generous gift of $RhCl_3 \cdot 3\ H_2O$. We thank E. Nadler, Institut für Physikalische Chemie, University of Tübingen,

for the scanning electron microscopy as well as Prof. K.G. Nickel, Institut für Mineralogie, University of Tübingen and Dipl.-Chem. Wolfram Wielandt, Institut für Anorganische Chemie, University of Tübingen, for BET measurements.

References

[1] E. Lindner, A. Baumann, P. Wegner, H.A. Mayer, U. Reinöhl, A. Weber, T. S. Ertel, H. Bertagnolli, J. Mater. Chem., submitted for publication.
[2] J. Hagen, in: Technische Katalyse, VCH, Weinheim, 1996, p. 70.
[3] M. Beller, B. Cornils, C.D. Frohning, C.W. Kohlpaintner, J. Mol. Catal. A 104 (1995) 17.
[4] C.D. Frohning, C.W. Kohlpaintner, in: B. Cornils, W.A. Herrmann (Eds.), Applied Homogeneous Catalysis with Organometallic Compounds, VCH, Weinheim, 1996, p. 29.
[5] D. Evans, J.A. Osborn, G. Wilkinson, J. Chem. Soc. A (1968) 3133.
[6] W. Wiebus, B. Cornils, Chem.-Ing.-Tech. 66 (1994) 916.
[7] P. Panster, S. Wieland, in: B. Cornils, W.A. Herrmann (Eds.), Applied Homogeneous Catalysis with Organometallic Compounds, VCH, Weinheim, 1996, p. 605.
[8] P. Hodge, Chem. Soc. Rev. 97 (1997) 417.
[9] F.R. Hartley, Supported Metal Complexes, Reidel, The Netherlands, Dordrecht, 1985.
[10] F.R. Hartley, P.N. Vezey, Adv. Organomet. Chem 15 (1977) 189.
[11] C.U. Pittmann, in: G. Wilkinson, F.G.A. Stone, E.W. Abel (Eds.), Comprehensive Organometallic Chemistry, Vol. 8, Pergamon, Oxford, 1982, p. 553.
[12] A.D. Pomogailo, Russ. Chem. Rev. 61 (1992) 133.
[13] F. Ciardelli, E. Tsuchida, D. Wöhrle (Eds.), Macromolecule–Metal Complexes, Springer, Berlin, 1996.
[14] M.G.L. Petrucci, A.K. Kakkar, Adv. Mater. 8 (1996) 251, and references therein.
[15a] E. Lindner, T. Schneller, F. Auer, H.A. Mayer, Angew. Chem. 111 (1999) 2288.
[15b] E. Lindner, T. Schneller, F. Auer, H.A. Mayer, Angew. Chem., Int. Ed. Engl. 38 (1999) 2154.
[16] U. Schubert, New J. Chem. 18 (1994) 1049.
[17] O. Kröcher, R.A. Köppel, A. Baiker, J. Chem. Soc., Chem. Commun. (1996) 1497.
[18] E. Lindner, M. Schreiber, T. Schneller, P. Wegner, H.A. Mayer, W. Göpel, C. Ziegler, Inorg. Chem. 35 (1996) 514.
[19a] H.A. Mayer, J. Büchele, in: H. Werner, P. Schreier (Eds.), Selective Reactions of Metal Activated Molecules, Vieweg, Braunschweig, 1998, p. 291.
[19b] J. Büchele, H.A. Mayer, Chem. Commun. (1999) 2165.
[20] E. Lindner, T. Schneller, H.A. Mayer, H. Bertagnolli, T.S. Ertel, W. Hörner, Chem. Mater. 9 (1997) 1524.
[21] E. Lindner, T. Schneller, F. Auer, P. Wegner, H.A. Mayer, Chem. Eur. J. 3 (1997) 1833.
[22] S. Wielandt, P. Panster, in: M.G. Scaros, M.L. Prunier (Eds.), Catalysis of Organic Reactions, Marcel Dekker, New York, 1996, p. 383.
[23] K.G. Allum, R.D. Hancock, I.V. Howell, R.C. Pitkethly, P.J. Robinson, J. Catal. 43 (1976) 322.
[24a] T. Okano, Y. Kobayashi, H. Konishi, J. Kiji, Bull. Chem. Soc. Jpn. 55 (1982) 2675.
[24b] E. Lindner, A. Bader, E. Glaser, B. Pfleiderer, W. Schumann, E. Bayer, J. Organomet. Chem. 355 (1988) 45.
[25a] E. Lippmaa, M. Mägi, A. Samoson, G. Engelhardt, A.-R. Grimmer, J. Am. Chem. Soc. 102 (1980) 4889.
[25b] E. Lippmaa, A. Samoson, Bruker Rep. 1 (1982) 6.
[26] J. Schaefer, E.O. Stejskal, R. Buchdahl, Macromolecules 10 (1977) 384.
[27] A.D. Torchia, J. Magn. Reson. 30 (1978) 613.
[28] T.S. Ertel, H. Bertagnolli, S. Hückmann, U. Kolb, D. Peter, Appl. Spectrosc. 46 (1992) 690.
[29] M. Newville, P. Livins, Y. Yakobi, J.J. Rehr, E.A. Stern, Phys. Rev. B 47 (1993) 14126.
[30] S.J. Gurmann, N. Binsted, I. Ross, J. Phys. C 19 (1986) 1845.
[31] G. Brauer, Handbuch der Präparativen Anorganischen Chemie, Ferdinand. Enke, Stuttgart, Germany, (1981) 1977.
[32] S.J. LaPlaca, J.A. Ibers, J. Am. Chem. Soc. 85 (1963) 3501.
[33] H.W. Oviatt Jr., K.J. Shea, J.H. Small, Chem. Mater. 5 (1993) 943.
[34] E. Lindner, M. Kemmler, H.A. Mayer, P. Wegner, J. Am. Chem. Soc. 116 (1994) 348.
[35] K. Schmidt-Rohr, H.W. Spiess, Multidimensional Solid State NMR and Polymers, Academic Press, London, 1994.
[36] A.A. Oswald, D.E. Hendriksen, R.V. Kastrup, E.J. Mozelski, Homogeneous Transition Metal Catalyzed Reactions, in: W.R Moser, D.W. Slocum (Eds.), Advances in Chemistry Series 230 ACS, Washington, DC, 1992, p. 395, Chap. 27.